Characterization and modelling of cure-dependent properties and strains during composites manufacturing

Laure Moretti, Bruno Castanié, Gérard Bernhart, Philippe Olivier

Characterization and modelling of cure-dependent properties and strains during composites manufacturing

Laure Moretti, Bruno Castanié, Gérard Bernhart and Philippe Olivier

Abstract

The geometric stability of structural parts is a critical issue in the aeronautical industry. However, autoclave curing of primary structural composite parts may cause significant distortions and divergences between the mould nominal geometries and the final shapes of the parts. To be able to anticipate such distortions, a robust simulation tool is needed, which can be implemented only if the phenomena involved are properly understood and characterized. The thermo-kinetic behaviour of the M21EV/IMA prepreg is fully characterized in this paper. Thermal strains and chemical shrinkages are measured using Thermo-Mechanical Analysis during the cure and the experimental method developed allows the thermo-chemical strains to be obtained even during the early stages of the cure. An experimental setup is developed to measure the thermo-mechanical behaviour of the material during its cure. Thanks to these measurements, a new constitutive mechanical model, inspired from the CHILE model, is defined. These data are then used as inputs for an FEA simulation of the entire curing process. Finally, the model is validated using the cure degree, glass transition and temperature monitoring, and post-cure distortion measurements.

Keywords

Autoclave, cure behaviour, thermosetting resin, process simulation

Introduction

Because of their specific properties, composite laminates made of carbon and thermosetting resins are very efficient materials for primary structural parts in aeronautics. However, their production remains costly and does not always provide satisfactory geometric stability.

During their cure, composite parts are subjected to several multi-physical phenomena, which may cause residual stresses and strains that will impact the final geometry of the part. The variations of geometry are critical for parts of large dimensions, where the displacements caused by small strains can be significant.

It is possible to compensate for such strains by modifying the initial mould. A jig-shaped mould is then built to obtain a part with the desired geometry after demoulding (see Figure 1). This mould geometry can be obtained by an iterative trial and error approach. However, this is time consuming and expensive, especially for parts of large dimensions. Therefore, efficient virtual manufacturing methods are needed to simulate and predict the cure strains and to produce the right compensated mould directly.

Nevertheless, the phenomena involved are numerous and complex. During the curing process, internal stresses are built up inside the composite part and will result in residual constraints. When the part is released from the mould, they are partially or fully relieved and distortions appear. The distortions can be of various kinds: spring-in, warpage, forced interaction and indirect distortions, as illustrated in Figure 2. Spring-in corresponds to a modification of angles and curved areas. Warpage is the distortion of areas that were originally flat. Some authors[1] also differentiate what they call forced interaction. This corresponds to a geometric locking of the part due to a mechanical action of the

Institut Clément Ader (ICA), Université de Toulouse, France

Corresponding author:
Bruno Castanié, INSA, 135 Avenue de Rangueil, Toulouse 31077, France.
Email: bruno.castanie@insa-toulouse.fr

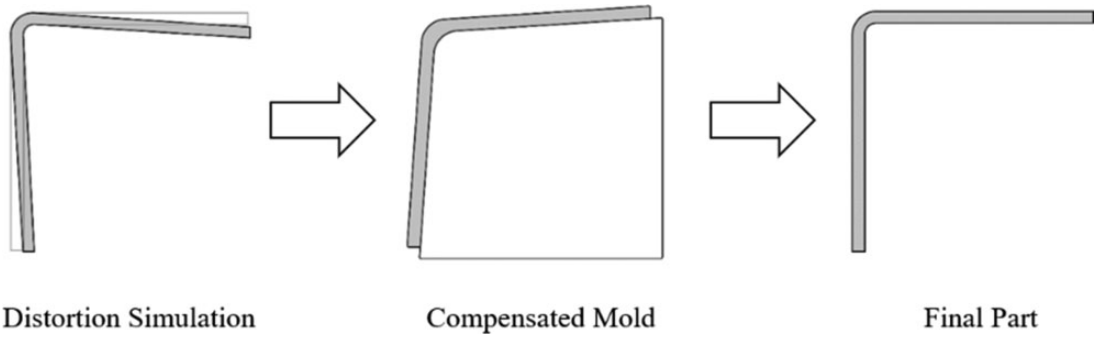

Figure 1. Compensated mould method.

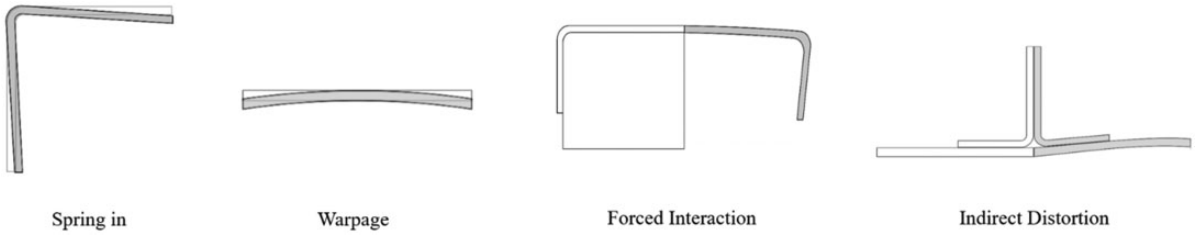

Figure 2. Different types of distortions of composite parts.

mould. In the case of assembled structures, indirect distortions can be caused by the transmission of strains between the different parts of the assembly.

It is possible to classify the parameters responsible for cure strains in two main groups: intrinsic and extrinsic parameters.[2] Intrinsic parameters are directly linked to the properties of the material or the geometry of the part and the main issues are thermal expansion and chemical shrinkage. The difference of coefficients of thermal expansion (CTE) between fibres and matrix, and thus between plies, depending on their orientation, will constrain the part during cure. The chemical shrinkage caused by the crosslinking of thermosetting resins will have the same kind of effects. Extrinsic parameters, on the other hand, are linked to external causes like the interaction with the tool or curing conditions.

One of the main challenges when simulating composite cure strains is to properly characterize the impacting material properties. Broadly speaking, these properties depend on the chemical state of the resin and, therefore, on its cure degree. The first step of this study will therefore characterize and accurately predict the thermokinetic behaviour of the material. Only then will it be possible to study the thermo-chemical and thermomechanical properties of the material.

The characterization of the thermal expansion or contraction and of the chemical shrinkage is crucial to properly describe cure strains. Various methods can be found in the literature to characterize their variations during curing. For example, some authors have used thermo-mechanical analysis on pre-cured samples.[3,4] This method gave satisfying results but is limited to post-gel measurements. Garstka et al. developed a device made of two heating plates to measure the through-the-thickness strain of a cross-ply laminate.[5] Plunger (PVT)-type dilatometers are also often used and developed[6,7]; they provide a dilatometric measurement for the complete curing process. However, the pressure used to conduct the test may affect the measurements. One last example of the various methods existing in the literature is the use of Fibre Bragg Grating sensors.[8–10] Those sensors, placed directly inside the composite part, allow to monitor strains during the industrial curing process. However, this method is limited to post-gel measurements. In this paper, an experimental method is developed to measure the thermal and chemical strains during the composite cure, even at the early stages of the crosslinking, using TMA.

Another challenging step of material behaviour characterization is the study of thermo-mechanical properties. Because of the low capability of resins to withdraw stresses before gel, the thermo-mechanical behaviour of polymeric composites during cure is hard to measure. The mechanical constitutive model of these materials is often approximated using post-cure measurements, but various authors have tried to set up experimental methods to measure the mechanical behaviour of composites during curing. Crasto and Kim used a rheometer to perform torsion tests during the curing of a graphite/epoxy prepreg.[11] Johnston applied the same kind of method to

measure the development of the mechanical properties of a carbon/epoxy prepreg.[12] Various authors have measured the thermo-mechanical behaviour of composites on pre-cured samples by dynamic mechanical analysis (DMA),[12–17] thus limiting the tests to post-gel behaviour. To fully characterize the development of mechanical properties during cure, a new experimental method is developed in this study. The data obtained are then used to define a new mechanical constitutive model inspired from the CHILE (Cure Hardening Instantaneous Linear Elastic) model.[18]

In the study presented here, significant characterization work is done to identify the thermo-kinetic, thermo-chemical and thermo-mechanical behaviours of the material throughout its cure. Various new experimental methods are put in place to measure the development of material strains and properties during cure. First of all, the thermo-kinetic behaviour is fully characterized. Then, the thermal and chemical cure strains are measured on uncured samples using thermo-mechanical analysis. Finally, the mechanical behaviour of the prepreg is studied. An experimental method is set up to measure the development of mechanical properties throughout the cure and a new constitutive model is developed. Based on this characterization work, a robust FEA model is implemented using FORTRAN user subroutines. The main outputs of the model are the complete thermo-kinetic state of the material (temperature, cure degree, temperature of glass transition), the mechanical moduli of the material and cure strains and stresses development during cure. Cure strains can be separated according to their origins: thermal, chemical or mechanical. Finally, the model is compared to experimental measurements for validation. These validations are done using cure degrees, glass transition and temperature monitoring, and post-cure measurements of distortions.

Material and experimental methods

Material and manufacturing

The research presented in this paper focuses on laminated structures made of a carbon/epoxy prepreg IMA/M21EV provided by Hexcel. The IMA/M21EV prepreg has the particularity of being toughened with thermoplastic nodules as illustrated in Figure 3. The nodules modify the properties of the material in its thickness. The composite obtained is thus fully orthotropic and does not have transversely isotropic properties.

The composite parts are manufactured through an autoclave process with a two-dwell cycle achieving 180°C at its highest dwell. INVAR moulds treated with FREKOTE 700C and protected with an FEP releasing film are used to manufacture the composite parts.

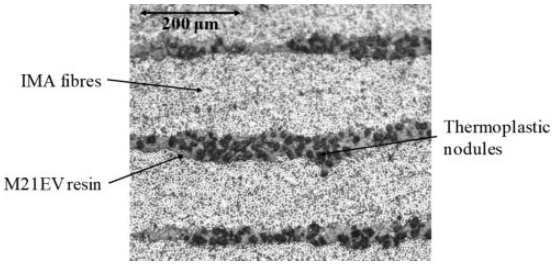

Figure 3. Image of the thickness of an M21EV/IMA laminate obtained by optical microscope.

This study is performed for primary structural parts that usually need to be assembled by bonding. During the bonding process, the composite part undergoes a new cure cycle. In this study, the cycle is identical to the first one, so most of the characterization and simulation works presented here take the material behaviour during, not one, but two consecutive cure cycles into account.

Differential scanning calorimetry

A TA Instruments differential scanning calorimeter (DSC) Q100 was used to measure the heat flow released during cure and the specific heat capacity evolution. The heat flow measured was used in order to study the influence of time and temperature on the crosslinking and on the physicochemical state of the resin. Dynamic and isothermal tests were run to characterize the kinetics and the glass transition temperature behaviour of the material. Samples in sealed aluminium pans filled with 23 ± 0.5 mg for the M21EV/IMA were used for all tests. Dynamic tests were performed with various heating ramps between 1°C/min and 20°C/min, starting at −50°C and going up to 350°C. Isothermal tests were also performed at various temperatures and during different periods. At the end of each isothermal dwell, a dynamic test was run with a heating ramp of 10°C/min. Each type of test was repeated at least three times. The DSC was calibrated with indium samples.

To enrich the DSC tests and to obtain the heat capacity behaviour law of the M21EV/IMA, modulated DSC tests were conducted using a heating ramp of 10°C/min. For these, the apparatus was calibrated with sapphire and indium. An amplitude of ±1°C and a frequency of 60s were used. All DSC tests are performed according to the standard ISO 11357.

Laser flash analysis

An experimental method was developed to obtain laser flash analysis (LSF) measurements during the curing of prepreg samples by means of a Netzsch LFA 457 MicroFlash. The sample support was protected by a

releasing agent (FREKOTE 700C). A 2°C/min ramp was imposed with isothermal dwells of 3 min at 25°C, 50°C, 75°C, 100°C, 125°C, 150°C, 175°C, 200°C, 225°C and 250°C. During each dwell, three measurements of diffusivity were made. Each uncured sample was submitted to this cycle twice in order to decorrelate the influence of cure degree from that of temperature on measurements. The first cycle allows to measure the variation of diffusivity for the uncured material and during cure. During the second cycle, the resin is fully cured, and the behaviour of the diffusivity for a cured material can be obtained. The tests measured the diffusivity of the material and the conductivity could then be deduced using equation (1)

$$\lambda(\alpha, T) = a(\alpha, T) \cdot Cp(\alpha, T) \cdot \rho(\alpha, T) \qquad (1)$$

where λ is the thermal conductivity, a is the diffusivity, Cp is the specific heat capacity and ρ is the density of the material.

Thermal mechanical analysis

Various thermal mechanical analyses (TMAs) were conducted on a Netzsch TMA 402 F3 Hyperion device in the aim of identifying the thermal expansion and the chemical shrinkage behaviour of the M21EV/IMA. For this purpose, an experimental method was developed. The M21EV/IMA being fully orthotropic, the measurements had to be made in every ply direction to obtain the thermo-chemical strain behaviour of the M21EV/IMA. To measure the strains in the thickness of the prepreg, samples of $3 \times 10 \times 10$ mm were cut from an uncured quasi-isotropic compacted laminate of 16 plies. To also obtain the thermo-chemical strains in each planar direction, samples of $6 \times 8 \times 8$ mm were cut from a unidirectional compacted laminate of 40 plies. The samples were placed between two layers of releasing film and positioned inside the TMA. A force of 1 mN was used to avoid any crushing of the samples during the cure. Three sets of experiments were performed:

- Isothermal dwells during which only the chemical strain acted. The samples were heated at 20°C/min from 20°C to 150°C. The isothermal dwell was maintained for 6 h.
- Slow ramps involving thermal and chemical strains. Once the chemical shrinkage effect had been subtracted from the total strain measured, the remaining strain was due only to the thermal effect. The various CTE were thus obtained from these measurements. A heating ramp of 1°C/min was used up to 300°C and cooled down to 20°C at the same rate. The cycle was repeated twice for each sample.
- Finally, a complete cure cycle was applied to validate the thermo-chemical behaviour identified.

Usual TMA measurements were also made on unidirectional cured samples to confirm the rubbery and vitreous CTEs and to ensure the consistency with results for uncured samples. The cured samples were subjected to a ramp of 2°C/min starting at 20°C and ending at 300°C. Cooling down took place at the same rate and the process was repeated twice for each sample. The specimens were tested in each of the three directions to obtain the thermo-chemical behaviour for all ply orientations.

Dynamic mechanical analysis

To characterize the mechanical behaviour of our materials, a Metravib DMA$^+$ 100 DMA instrument was used. The usual method consists of loading the material at various iso-frequencies while applying a thermal ramp. When the cured material deteriorates with rising temperature, the mechanical properties fall to a low value. The experimental data are then used to identify the parameters of the mechanical constitutive model. However, even though the mechanical behaviour of materials during cure can be extrapolated from those results, the uncured properties are not fully characterized. A cured thermosetting epoxy will never return to its initial state. To be able to identify the constitutive mechanical law on the actual behaviour of the uncured material, tests must be achieved on uncured specimens. An experimental methodology was set up to measure the development of mechanical properties using a DMA, not on precured samples, but on fully uncured samples.

Firstly, uncured samples of $0.6 \times 10 \times 40$ mm of [+45/−45/+45] laminates were tested dynamically. The clamps of the DMA were protected by FEP release film. The samples being soft, the tensile dynamic stress was fixed for a displacement at 3×10^{-6} m. The tests were performed with an applied iso-frequency of 1 Hz. Three kinds of tests were performed: thermal ramps of 1°C/min and 2°C/min from 20°C up to 220°C, one cure cycle followed by a thermal ramp of 2°C/min from 20°C up to 300°C, and two cure cycles followed by a thermal ramp of 2°C/min from 20°C up to 300°C.

Secondly, uncured quasi-isotropic samples of $3 \times 10 \times 10$ mm were tested by applying dynamic compression. Once again, the apparatus was protected by a releasing film. A compression static effort of 10 N and a dynamic effort of 2 N were applied. The tests were performed with an iso-frequency of 1 Hz. The sample was subjected to two cure cycles followed by a thermal ramp of 2°C/min from 20°C up to 300°C.

Finally, usual tests were performed on cured samples to check the consistency of the results. Cured samples

were cut from a unidirectional laminate and tested in the three directions. The tests were performed at 1 Hz and with a dynamic displacement of 3×10^{-6} m. A thermal ramp of 2°C/min from 20°C/min up to 300°C/min was applied.

Experimental results

Thermo-kinetics

As mentioned before, the main properties of the epoxy matrix, and therefore of the composite, depend on the state and cure degree of the resin, so it is compulsory to be able to simulate its chemical and thermal state during the cure. The crosslinking reaction being exothermic, there is a strong dependence between temperature and degree of cure. This is modelled by the heat equation derived from Fourier's law and from the conservation of energy principle (see equation (2))

$$\rho_c \, Cp_c \, \frac{\delta T}{\delta t} = div(\lambda_c(T) \cdot gradT) + \rho_m \, \Delta H_{tot} \, V_m \frac{\mathrm{d}\alpha}{dt} \quad (2)$$

where ρ_c is the density of the composite, Cp_c is its specific heat capacity, λ_c is the thermal conductivity tensor of the composite, ρ_m is the density of the resin, ΔH_{tot} is the total enthalpy of the resin, V_m is the volume fraction of matrix in the material, T is the temperature and $d\alpha/dt$ is the crosslinking rate.

A thermo-kinetic model is then needed to predict the temperature and the degree of cure of the material at any point of the parts and at any time during the cure. Associated laws and parameters must be identified.

Kinetics. Two kinds of kinetic models can be used: phenomenological models and mechanistic models. Phenomenological models describe the cure reaction in an empirical way. They ignore the details of reaction involved for each component of the material. In contrast, mechanistic models accurately follow every chemical reaction contributing to the cure of the resin. They are extremely complex models in which the work required to characterize and identify parameters is considerable.[15] Therefore, phenomenological models are largely preferred for the study of the M21EV type of epoxy resins.[15,19–22]. Usual phenomenological models for these thermosets are the Bailleul model[15] and the modified Kamal Sourour model.[19–21] Relying on Paris's comparison of these models[21,23] on M21E, the modified Kamal Sourour model was used. The behaviour law is described by equations (3) and (4)

$$\frac{\mathrm{d}\alpha}{dt} = (k_1 + k_2 \cdot \alpha^m)(\alpha_{max} - \alpha)^n \quad (3)$$

$$k_i = A_i \cdot \exp\left(-\frac{E_{a_i}}{R \cdot T}\right) \quad \text{and} \quad i = 1, 2 \quad (4)$$

where α is the cure degree, $d\alpha/dt$ is the crosslinking rate, α_{max} is the maximum cure degree and m and n are constants. k_1 and k_2 are the apparent reaction rates of the crosslinking, they increase with the temperature following the Arrhenius relationship described in equation (4). A_i is a pre-exponential constant, E_{a_i} is the activation energy and R is the universal gas constant.

Maximum cure degree. To determine its maximum cure degree behaviour, samples of M21EV/IMA were subjected to DSC isothermal analysis following the method described in the 'Experimental methods' section. Residual enthalpies obtained were compared to the ΔH_{tot} of the complete cure reaction. Measured on thermal ramp of 10°C/min, the total enthalpy of reaction ΔH_{tot} has a value of 144.3 ± 2.3 J/g for the prepreg. Using the volume fraction of fibre, the enthalpy of the neat resin should be 429.6 ± 7.0 J/g. This value is in line with the measurements done by C. Paris et al.[23] obtained a total enthalpy of 424 J/g for the neat resin M21. Maximum degrees of cure were obtained for various isotherms, using equation (5). A polynomial law was chosen to describe the evolution of the maximum degree of cure

$$\alpha_{max} = 1 - \frac{\Delta H_{resi}}{\Delta H_{tot}} \quad (5)$$

Kamal Sourour parameters. The various parameters of the modified Kamal Sourour law were identified thanks to a Matlab algorithm. The algorithm identifies the parameter values that minimize the gap between experimental results and the Kamal Sourour law. The main Matlab functions used are lsqnonln associated with a multistart. lsqnonln is a non-linear least-square solver and multi-start can launch the algorithm from a multitude of initial values. This method is used to avoid any local minimum and to ensure that the parameters identified are those corresponding to the global minimum between experimental results and the Kamal Sourour law. The algorithm was applied to all isothermal and dynamic DSC tests presented in the 'Experimental methods' section. The Matlab algorithm identified m, n, k_1, k_2 for various isotherms. Confrontations of model results with experimental data are illustrated in Figures 4 and 5. Despite some deviations for high heating rates, the precision of the modified Kamal Sourour model identified is sufficient here. Indeed, the highest heating rate of the industrial curing cycle used in this research project is 1.5°C/min and the accuracy of the model at these rates is satisfactory.

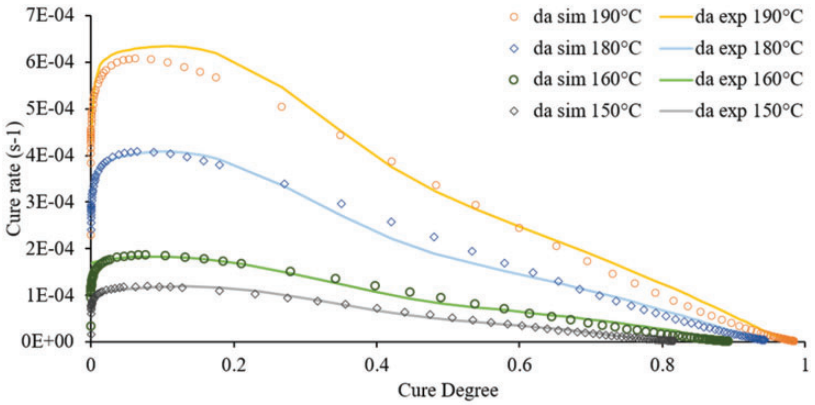

Figure 4. Comparison between differential scanning calorimeter isothermal measurements and model predictions of the cure degree.

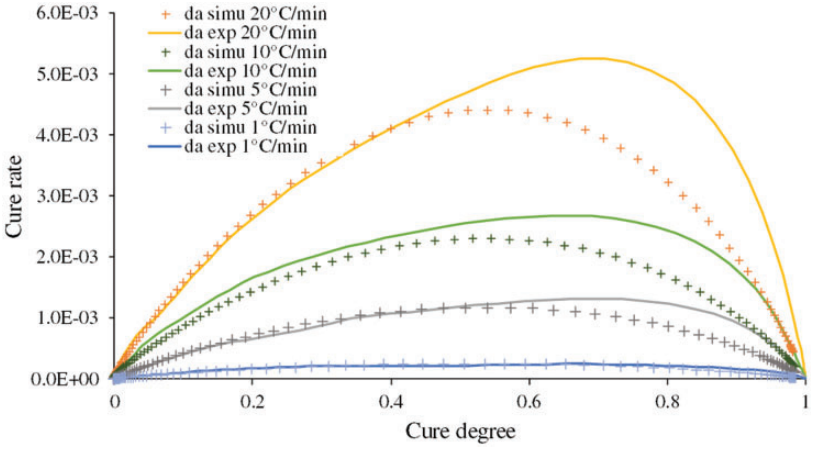

Figure 5. Comparison between differential scanning calorimeter dynamic measurements and model predictions of the cure degree.

Glass transition. To describe the evolution of glass transition during the cure of an epoxy resin, one of the models most frequently used in the literature[15,20–22] is the Di Benedetto model. This model, developed by Di Benedetto and modified by Pascault and Williams,[24–27] is described by equation (6). Parameters of the Di Benedetto law are identified, thanks to a GRG nonlinear solver on Excel with a 10,000 multistart. The solver minimizes the square gradient $\left(T_g^{exp} - T_g^{sim}\right)^2$.

$$\frac{T_g - T_{g0}}{T_{g\infty} - T_{g0}} = \frac{p \cdot \alpha}{1 - (1-p) \cdot \alpha}$$

p is an adjustable parameter, and $T_{g\infty}$ and T_{g0} are the glass transition temperatures of the completely reacted and un-cured resin, respectively.

Thermal properties

Specific heat capacity. The specific heat capacity, noted *Cp*, represents the energy needed to heat up a unit mass of a material by 1°C (or Kelvin). A mixture law was used to describe the evolution of *Cp* (see equation (7)). The behaviour of the *Cp* for the uncured and cured resin was identified by various dynamic measurements by modulated DSC, as described in the experimental methods section. $Cp_{cured}(T)$ and $Cp_{uncured}(T)$ behaviours could be fitted linearly for both materials as described by equations (8) and (9)

$$Cp(\alpha, T) = Cp_{cured}(T) \cdot \alpha + Cp_{uncured}(T) \cdot (1-\alpha) \quad (7)$$

$$Cp_{cured}(T(^\circ C)) = 2.439 \cdot T + 598.7 \quad (8)$$

$$Cp_{uncured}(T(^\circ C)) = 1.990 \cdot T + 725.0 \quad (9)$$

Diffusivity and conductivity. The diffusivity of the prepreg was measured by LSF. The conductivity, noted λ, was then calculated using equation (1). Once again, measurements were made at various temperatures on cured and uncured samples. To describe the evolution

of conductivity during the cure, a mixture law was used (see equation (10)). Again, a linear law could be defined to describe $\lambda_{cured}(T)$ and $\lambda_{uncured}(T)$ behaviours

$$\lambda(\alpha, T) = \lambda_{cured}(T) \cdot \alpha + \lambda_{uncured}(T) \cdot (1 - \alpha) \quad (10)$$

Thermo-chemical strains

Cure strains have three main origins: thermal, chemical and mechanical. Thermal strains are due to the CTE involved during the cure. Such strains are directly linked to the temperature increment (see equation (11)). Chemical strains, on the other hand, are due to chemical shrinkage of the resins that occurs during crosslinking. This shrinkage can be modelled using equivalent expansion coefficients linked to the increment of cure degree (see equation (12)). The equivalent CTE is named coefficient of chemical shrinkage (CCS). Both coefficients are dependent on the chemical state of the resin as described by equations (13) and (14)

$$\Delta\varepsilon^{therm} = CTE \cdot \Delta T \quad (11)$$

$$\Delta\varepsilon^{chem} = CCS \cdot \Delta\alpha \quad (12)$$

$$CTE_i = \begin{cases} CTE_i^{sup\,T_g} & T \geq T_g(\alpha) \quad \text{and} \quad i = 1,2,3 \\ CTE_i^{inf\,T_g} & T < T_g(\alpha) \quad \text{and} \quad i = 1,2,3 \end{cases} \quad (13)$$

$$CCS_i = \begin{cases} CCS_i^{bf\,gel} & \alpha < \alpha_{gel} \quad \text{and} \quad i = 1,2,3 \\ CCS_i^{af\,gel} & \alpha \geq \alpha_{gel} \quad \text{and} \quad i = 1,2,3 \end{cases} \quad (14)$$

where T_g is the glass transition temperature and α_{gel} is the cure degree at which the gelation occurs, and $i = 1,2,3$ are the three main directions of a prepreg ply as illustrated in Figure 6.

As explained before, the thermo-chemical strains were studied through TMA measurements on cured and uncured samples. Isothermal dwells, slow ramps and complete cure cycles were applied to prepreg samples. The results obtained for the isothermal dwells are illustrated in Figure 7. The strain, driven only by the chemical shrinkage, is plotted versus the cure degree. The cure degree was obtained using the modified Kamal Sourour model identified and the temperature measured during the test. As expected, the behaviour of the chemical shrinkage follows a bilinear law as a function of the cure degree. A slope change can be observed with the gelation of the resin. The chemical shrinkage is thus described by two CCS, before and after gel, as defined in equation (14). Following the same pattern, the thermal expansion and contraction was identified on slow thermal ramps. The computed chemical strain was subtracted from the total strain measurements, leaving only the thermal effect. As expected, its behaviour follows a linear law as a function of the temperature with a slope change at the glass transition temperature (see equation (13)).

Finally, the thermo-chemical strains were measured on a complete cure cycle, as illustrated in Figure 8. During the heating ramps, the resin passed through its viscous and rubbery states. The main effect impacting the strains during the ramps was the thermal expansion linked to the $CTE_i^{sup\,T_g}$, as illustrated in Figure 8(a). During the cooling down phase, a change of slope could be observed with the glass transition. There was no thermal effect over the two isotherms and the chemical shrinkage could be observed. The strain plotted as a function of the cure degree in Figure 8(b) illustrates the different slopes before and after gelation. The CTE and CCS obtained on the various ramps and isotherms of the cycle are concordant with the other results obtained on cured and uncured samples.

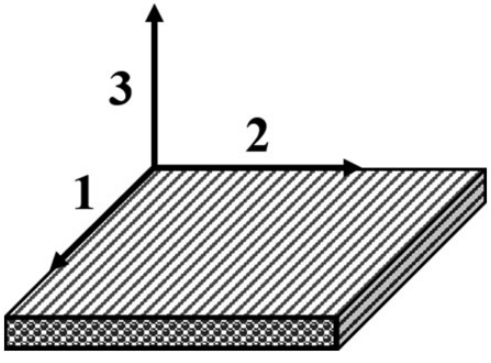

Figure 6. Illustration of directions of a prepreg ply.

Mechanical constitutive law

CHILE

Various mechanical constitutive models exist to describe the mechanical behaviour of epoxy resins. They can be divided into three main categories: thermoelastic, instantaneous elastic and viscoelastic. An epoxy resin, as studied here, has a viscoelastic time and temperature dependent behaviour. However, those models are time consuming, costly and need a large amount of characterization work. The model most often used to avoid these costs is the CHILE model. The properties of the epoxy resins considered evolved during the cure simulation but kept supposedly linear elastic behaviour at any given instant. Initially developed by Bogetti and Gillespie[28] in 1992, the model was then modified by Johnston et al.[18] In this version of the model, now frequently used, the authors added a temperature

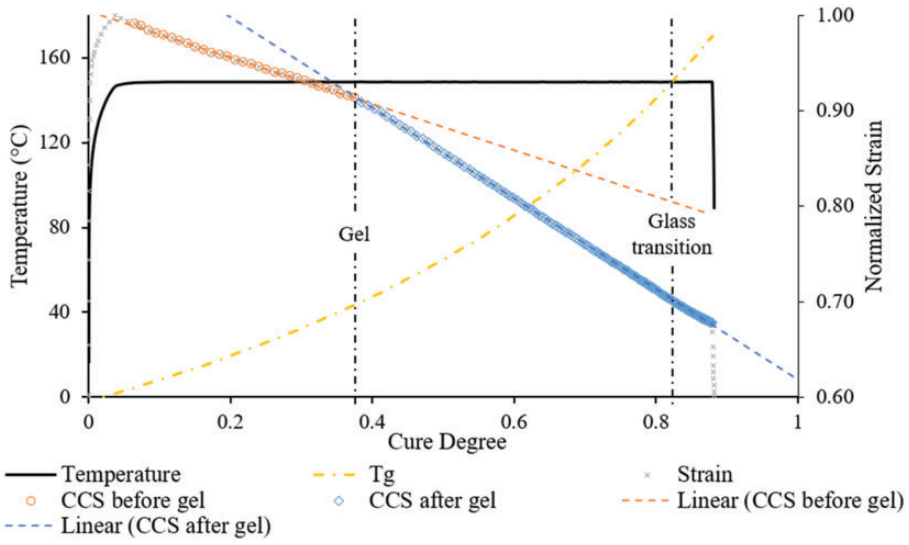

Figure 7. M21EV/IMA strain measured by thermal mechanical analyses during a 150°C isotherm.

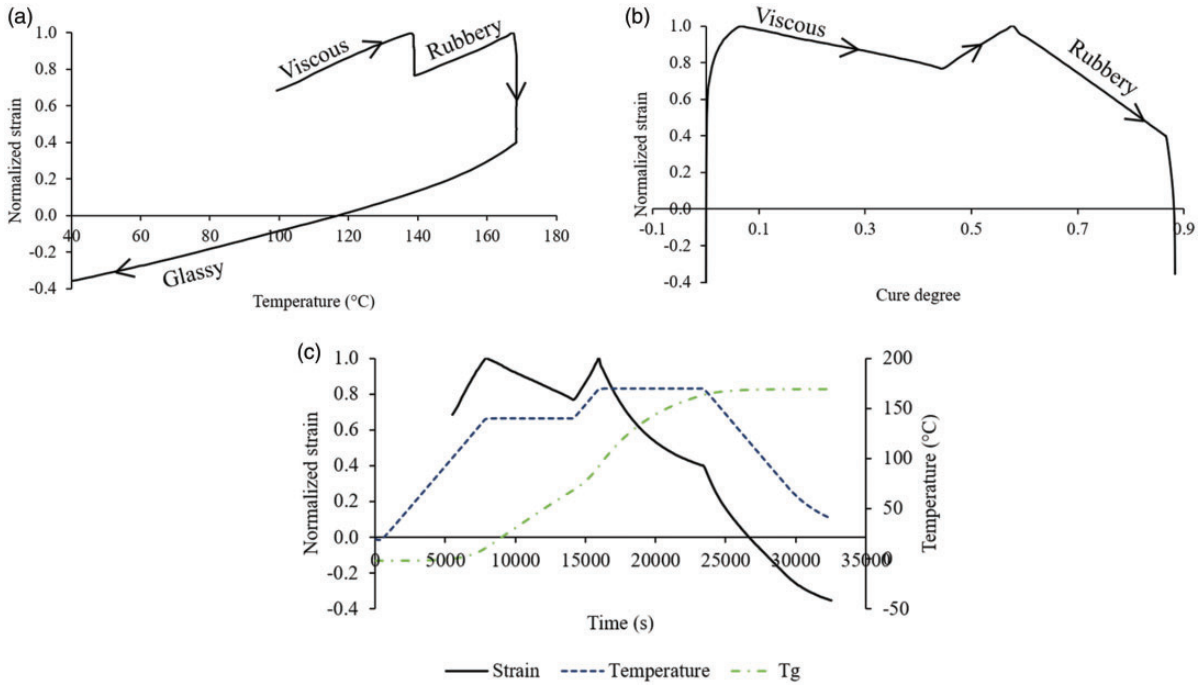

Figure 8. M21EV/IMA strain measured by thermal mechanical analyses during a cure cycle: (a) strain (*T*), (b) strain (α) and (c) strain (*t*).

dependency for the elastic constants of the resin. The CHILE model is defined by equations (15) and (16)

$$E = \begin{cases} E_1 & \text{if} \quad T^* < T^*_{C1}, \\ E_1 + \frac{T^* - T^*_{C1}}{T^*_{C1} - T^*_{C2}} \cdot (E_1 - E_2) & \text{if} \quad T^*_{C1} \le T^* < T^*_{C2}, \\ E_2 & \text{if} \quad T^* > T^*_{C2} \end{cases} \tag{15}$$

$$T^* = T_g - T = \frac{\lambda_{Tg} \cdot \alpha}{1 - (1 - \lambda_{Tg}) \cdot \alpha} \cdot (T_{g\infty} - T_{g0}) + T_{g0} - T \tag{16}$$

E_1 is the un-relaxed modulus, it corresponds to the cure state of the modulus at $T \ll T_g$; E_2 is the relaxed modulus at $T \gg T_g$; T^* is the difference between resin

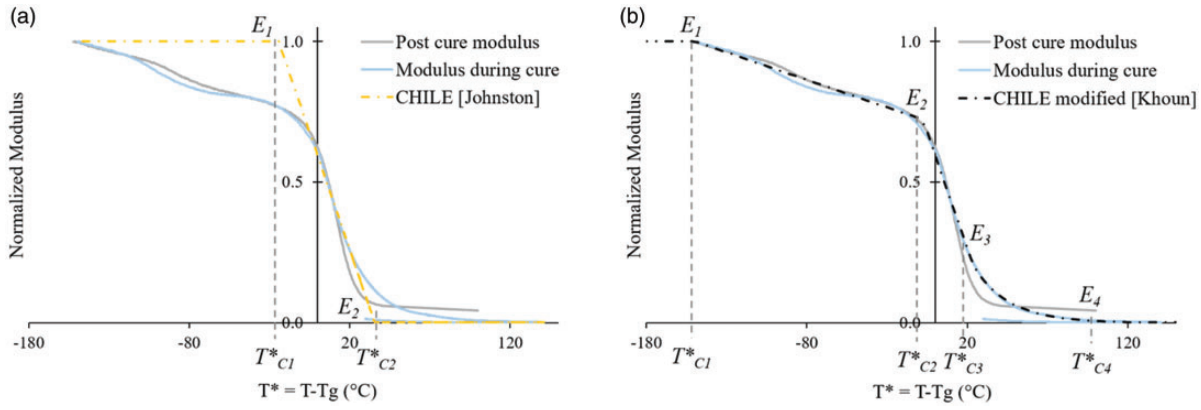

Figure 9. Comparison between experimental measurements and CHILE simulations of the M21EV/IMA transverse modulus behaviour: (a) CHILE and (b) modified CHILE. CHILE: Cure Hardening Instantaneous Linear Elastic model.

temperature and the instantaneous resin glass transition temperature. Replacing T_g with the Di Benedetto model developed before yields equation (16). T^*_{C1} and T^*_{C2} are the critical values of T^* at the end and at the beginning of vitrification.

Modified versions of Johnson's CHILE model were proposed by Khoun[29] and Curiel and Fernlund[30] to come closer to the modulus development during cure. Those modifications gave the mechanical constitutive equation (17)

$$E = \begin{cases} E_1 & \text{if } T^* < T^*_{C1}, \\ E_1 + \frac{T^* - T^*_{C1}}{T^*_{C1} - T^*_{C2}} \cdot (E_1 - E_2) & \text{if } T^*_{C1} \le T^* < T^*_{C2}, \\ E_2 + \frac{T^* - T^*_{C2}}{T^*_{C2} - T^*_{C3}} \cdot (E_2 - E_3) & \text{if } T^*_{C2} \le T^* < T^*_{C3}, \\ A \cdot exp(-K \cdot T^*) & \text{if } T^*_{C3} \le T^* < T^*_{C4}, \\ E_4 & \text{if } T^* > T^*_{C4} \end{cases} \tag{17}$$

where E_1, E_2, E_3, E_4, T^*_{C1}, T^*_{C2}, T^*_{C3}, T^*_{C4}, A and K are fitting constants.

DMA measurements. As explained before, DMA measurements were made on cured and uncured laminates of M21EV/IMA. To identify the parameters of the CHILE model, the DMA results were plotted as a function of T^* (see equation (16)). The modulus evolution is illustrated in Figure 9 and the two CHILE models presented in equations (15) and (17) are compared.

The modified CHILE model used by Khoun is better suited to the M21EV/IMA mechanical behaviour. However, as expected for a thermosetting resin based material, the modulus of the material had different behaviours during and after cure. This change of behaviour is not described by either of the two CHILE models presented here. To get closer to the measured behaviour of the M21EV/IMA, a new mechanical constitutive model was developed.

The behaviour can be divided into three domains, as illustrated in Figure 10. In domain 1, the material leaves its prepreg 'B stage'. The linearization of epoxy matrix chains induces a modulus decrease. Then, during domain 2, crosslinking begins and the mechanical properties start to develop. At the end of the cure (domain 3), the composite possesses its cured mechanical properties. Once this state has been reached, the thermosetting resin will never return to its initial state. A new model is then developed to describe these three steps. Behaviour laws and parameters are thus identified thanks to a MATLAB optimization algorithm following the modified CHILE model described in equation (17) for each of the three steps. The comparison between the DMA measurements and each CHILE model presented are illustrated in Figure 11. This figure shows the results obtained for a two cycle test followed by a thermal ramp. The best fit is obtained with the new CHILE model developed, which separates the behaviour before, during and after cure.

Model construction and validation

Global architecture of the model

The FEA model developed was implemented on Abaqus through FORTRAN user subroutines. The model can be divided into two modules as described in Figure 12. The thermo-kinetic module relies on a HETVAL subroutine. HETVAL allows the thermo-kinetics to be resolved and updates the cure degree, cure rate, heat flux, and glass transition. A USDFLD subroutine is used to define the cure degree and the temperature as fields, which are then used to compute the specific heat capacity and conductivity of the material during cure. Material properties computed by the thermo-kinetic module are used as input for the strain and stress module. This module is built on two

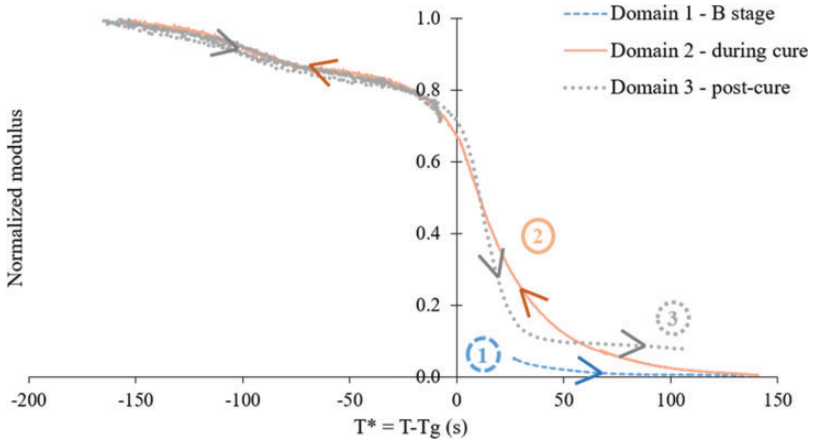

Figure 10. The three domains of the modified Cure Hardening Instantaneous Linear Elastic model developed.

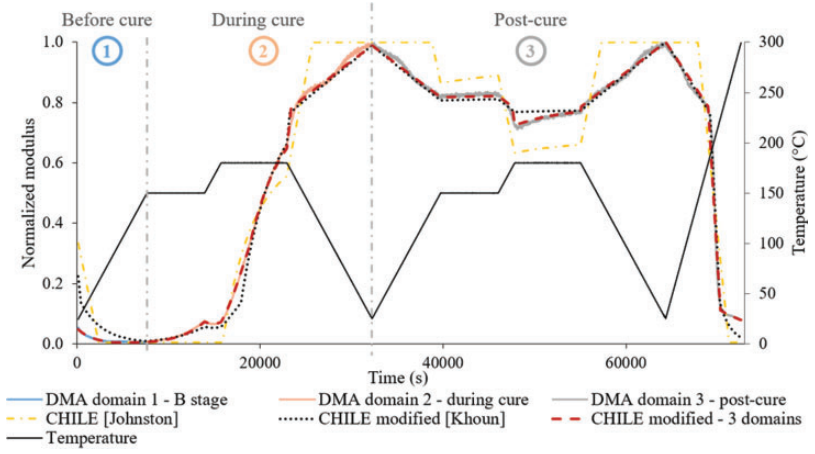

Figure 11. Comparison between experiment and simulation for the M21EV/IMA transverse modulus development during cure.

subroutines and relying on equations (18) to (20)

$$\Delta\varepsilon_{ij}^{tot} = \Delta\varepsilon_{ij}^{therm} + \Delta\varepsilon_{ij}^{chem} + \Delta\varepsilon_{ij}^{mech} \tag{18}$$

$$\Delta\sigma_{ij} = J_{ijkl} \cdot \Delta\varepsilon_{kl}^{mech} \tag{19}$$

$$\varepsilon_{ij}^{n+1} = \varepsilon_{ij}^{n} + \Delta\varepsilon_{ij}^{n} \tag{20}$$

where $\Delta\varepsilon_{ij}^{tot}$ is the total incremental strain composed by the incremental thermal strain $\Delta\varepsilon_{ij}^{therm}$, the incremental chemical strain $\Delta\varepsilon_{ij}^{chem}$ and the incremental mechanical strain $\Delta\varepsilon_{ij}^{mech}$. $\Delta\sigma_{ij}$ is the incremental stress component, J_{ijkl} is the material Jacobian matrix component and n denotes the time increment.

A UEXPAN subroutine computes the thermal and chemical strains, whereas a UMAT subroutine computes the development of the moduli during cure and the associated Jacobian matrix. Using these two subroutines, the strain and stress module is able to compute cure strains, stresses and displacements. The model is developed to be able to separate the strain according to its origin (thermal, chemical or mechanical). The model works in 2D and in 3D.

Thermokinetics validation

Kinetics and glass transition validation. DSC measurements were done at various steps of the cure cycle to validate T_g and cure degree simulations. Comparison between experimental and simulation results for T_g are illustrated in Figure 13. It can be seen that the thermo-kinetics model accurately predicts the cure degree and glass transition evolution during the two consecutive cure cycles.

Thermokinetics validation on thick parts. To validate the thermo-kinetics model on thick parts, a unidirectional

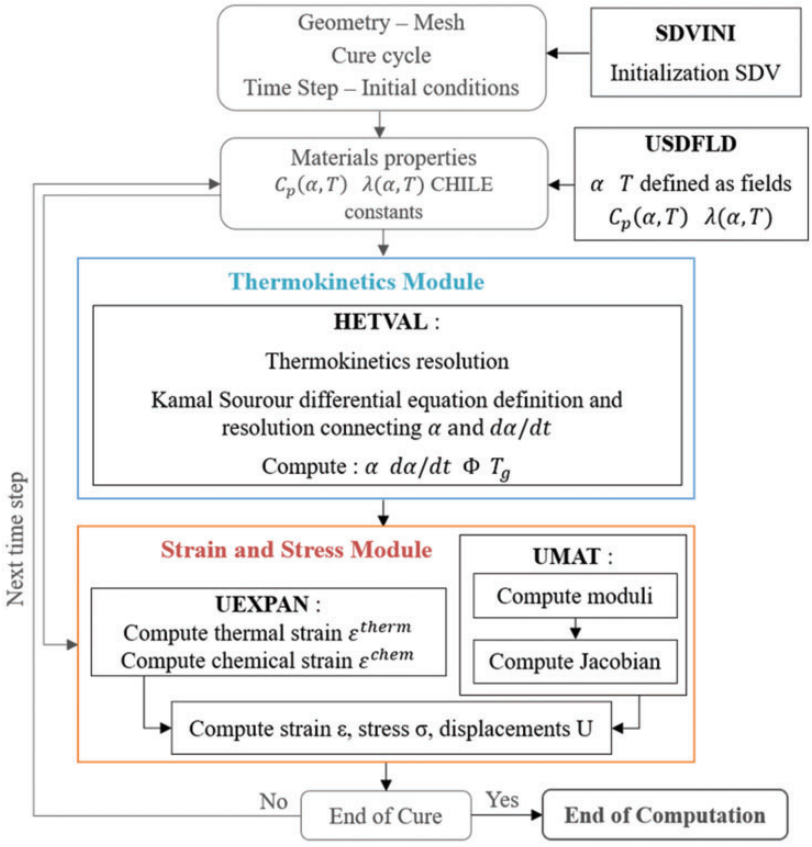

Figure 12. Global architecture of the FEA model.

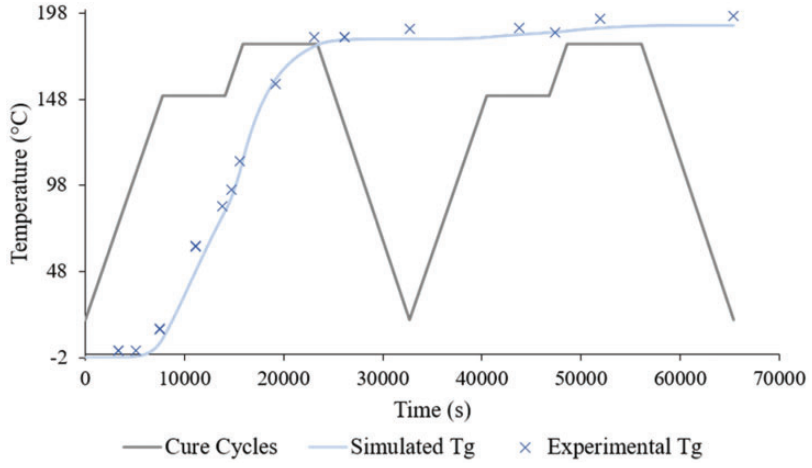

Figure 13. Comparison between experimental data and the FEA simulation of T_g evolution during two consecutive cycles.

laminate of 200 plies was instrumented with thermocouples and cured in an oven. The thermocouples were placed as illustrated in Figure 14:

- TC 1–2: between the first and the second ply at the centre of the part
- TC 49–50: between the 49th and the 50th ply at the centre of the part
- TC 100–101 C: between the 100th and the 101st ply at the centre of the part
- TC 100–101 B: between the 100th and the 101st ply at the edge of the part

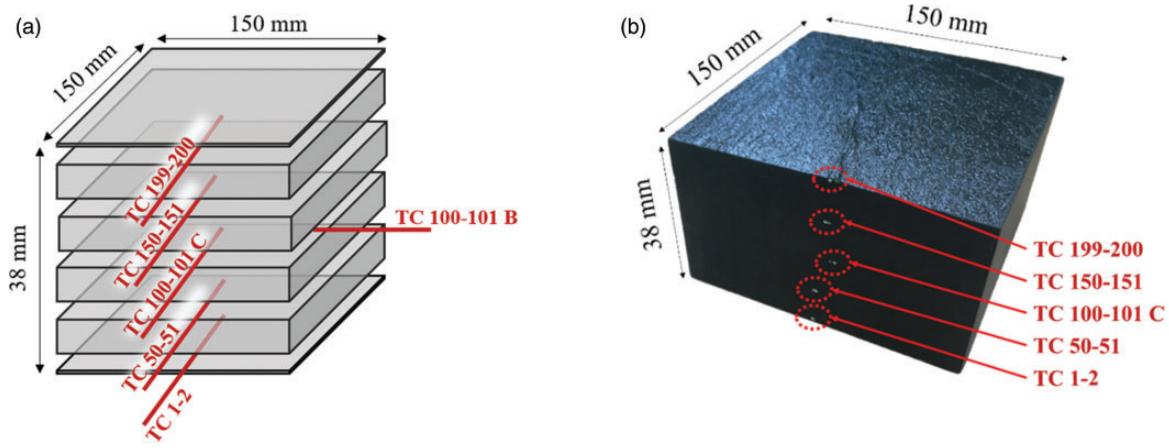

Figure 14. Experimental instrumentation of the thick laminate: (a) experimental set-up and (b) final part picture.

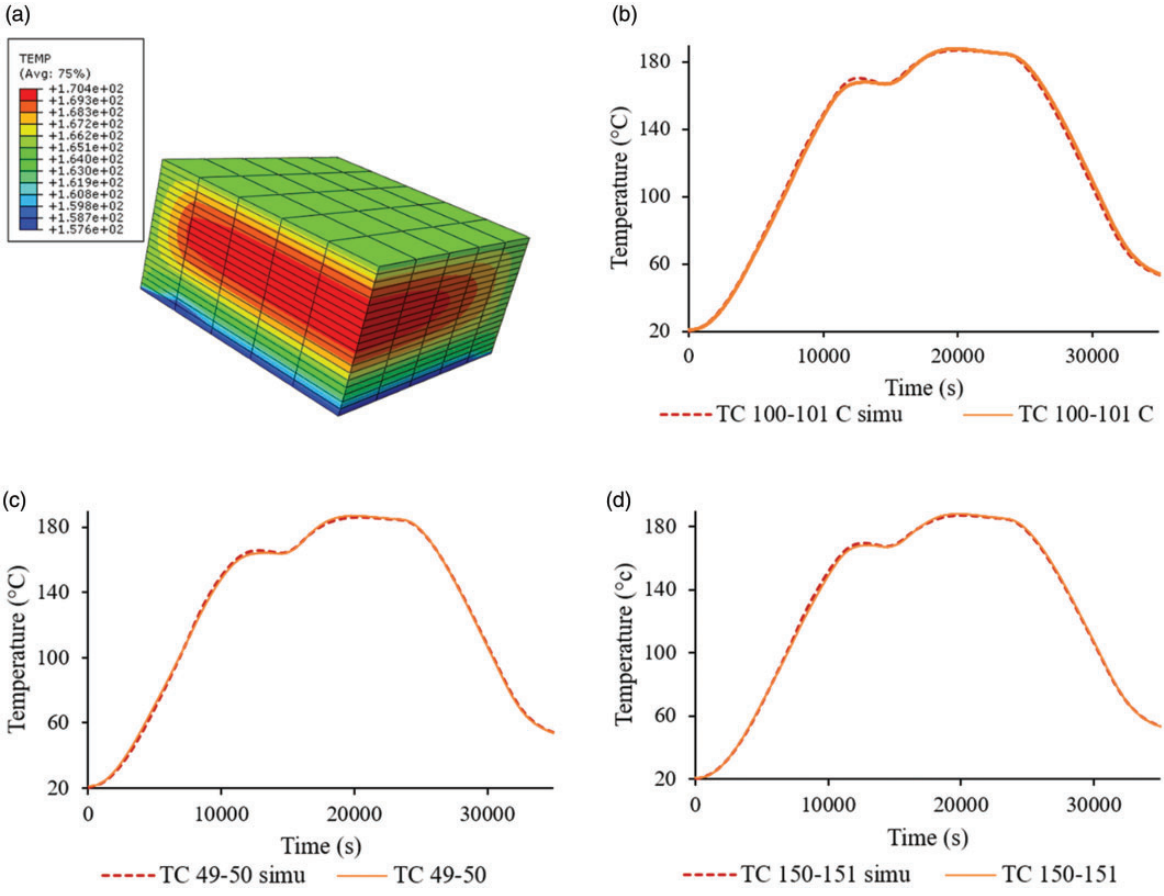

Figure 15. Comparison between thermal monitoring and cure simulation at the core of the thick laminate: (a) overshoot simulation during the first isothermal dwell, (b) TC 100–101 C versus simulation, (c) TC 49–50 versus simulation and (d) TC 150–151 versus simulation.

- TC 150–151: between the 150th and the 151st ply at the centre of the part
- TC 199–200: between the 199th and the 200th ply at the centre of the part

Two thermocouples were added to this instrumentation, one on the mould and another on the top of the composite part. Curing was simulated by applying experimentally measured temperatures at the top and

at the bottom of the structure. This method was justified since the cure process is controlled using those two thermocouples.

To reduce computation time and cost, only one quarter of the plate was modelled using symmetry conditions. At this step of the validation process, the aim was to verify the accuracy of the thermo-kinetic model alone. The composite part is thus meshed using DC3D8 elements. The thickness of the composite part is meshed with 20 elements, as illustrated in Figure 15(a).

The maximum error obtained when comparing the simulation with the experimental data measured by the thermocouples was 1.4%. It was measured during the overshoot of the first dwell of the cure cycle, at the core of the part. Figure 15 compares the data collected by the thermocouple TC 100–101 C, located at the core of the part, the thermocouple TC 150–151 and the thermocouple TC 49–50 with the simulation results at the corresponding nodes.

Final model validation

In order to validate the model, post cure distortion measurements were performed on various generic samples. Three kinds of corners were tested: $[90_{20}]$, $[0_{20}]$, and $[+45/-45/+45/-45/+45/-45/+45/-45/+45/-45]_s$. Two kinds of asymmetrical plates were also manufactured. The first was made of 20 plies of 300×150 mm and the second of 20 plies of 150×150 mm.

Post-cure distortions are measured by stereocorrelation using a speckle pattern. Two set of cameras Pike F-505B/F505-C provided by Allied Vision are used for measurements. The 3D profile of each specimen is reconstructed using VIC3D software.

To validate the model, the experimental measurements by stereocorrelation are compared with the simulated distortions. The various parts are meshed using C3D20T quadratic elements. The thickness of the parts is meshed with one element per ply. When allowed by the geometry of the part and the orientations of the plies, symmetry conditions are used to reduce the model cost. The simulation is divided in two steps: one step for the cure cycle of the composite part and one step for the demoulding of the part. The Invar mould is also modelled as illustrated in Figure 14. In the current model, the mechanical interaction between the mould and the composite part is ignored and a frictionless contact is used at the interface.

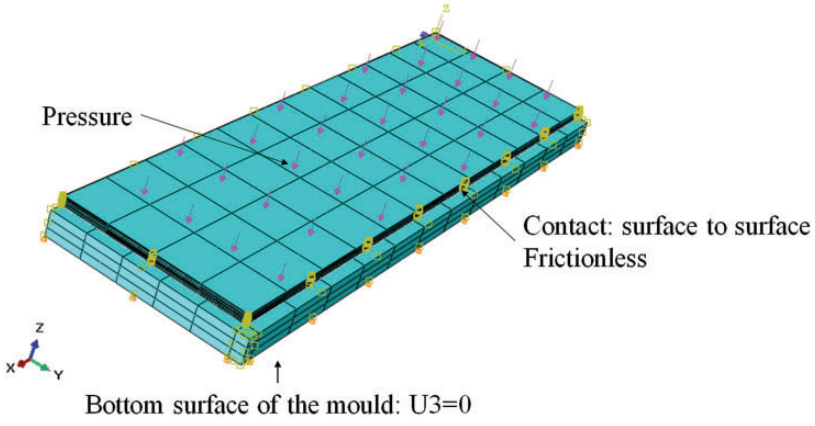

Figure 16. Asymmetrical plate model and mesh.

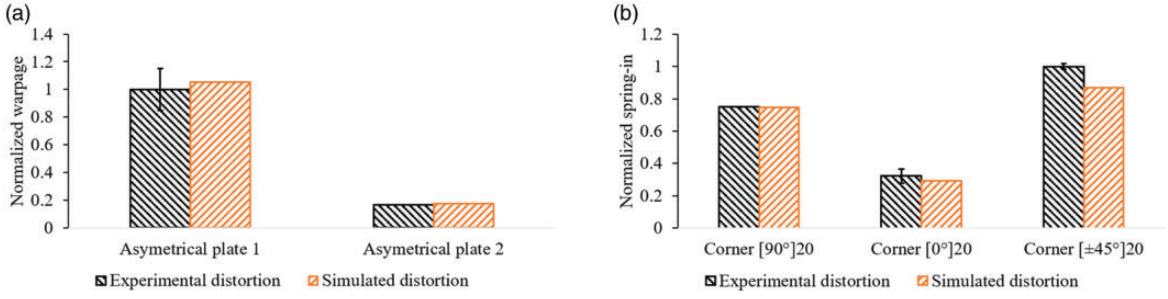

Figure 17. Confrontation between experimental distortion and simulated distortions for all generic cases: (a) plates and (b) corners.

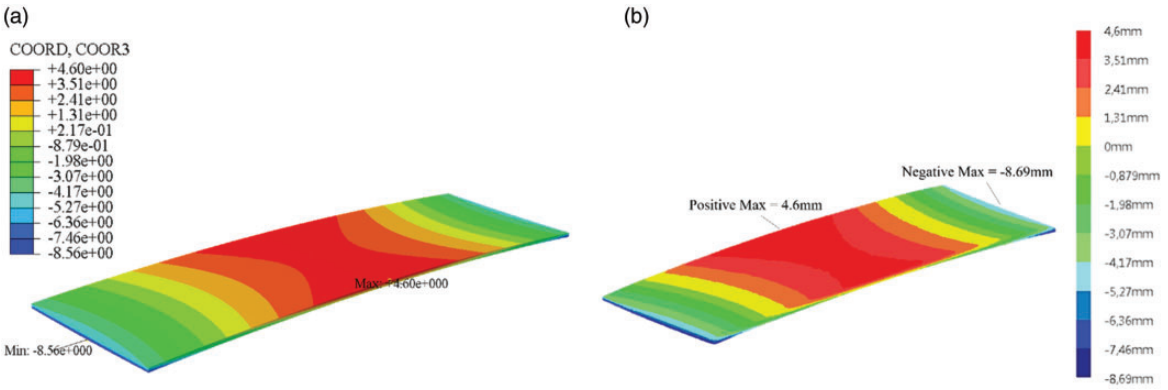

Figure 18. Confrontation between simulated and experimental distortion for asymmetrical plate 1: (a) simulation and (b) stereocorrelation.

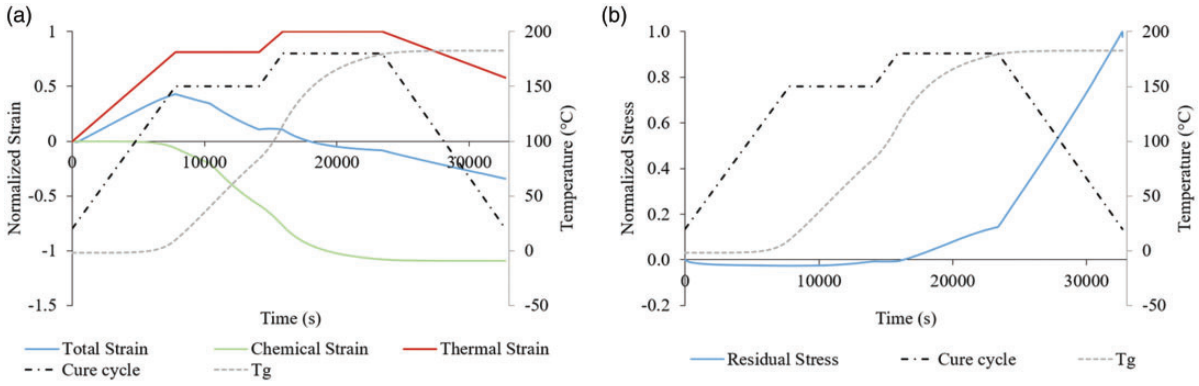

Figure 19. Simulation of development of thickness strains and transverse stresses at the centre of asymmetrical plate 1: (a) thickness strains and (b) transverse residual stresses.

The experimental measurements are compared with the simulated distortions in Figure 17. For the corners, the comparison was made on the spring-in value, and, for the plates, it concerned the warpage. The results presented in Figure 14 show that the model predicts the distortions with satisfactory accuracy. Of course, distortion distribution on each part is also compared with simulation, as illustrated in Figure 18.

In addition, the model developed allows strain simulations to be separated according to their origins: thermal, chemical or mechanical. The simulation thickness strain development during the cure of asymmetrical plate 1 is illustrated in Figure 19. The figure also shows the evolution of residual transverse stresses during the cure. As expected, at the beginning of the cure, stresses remain low, essentially because of the low modulus of the resin. After gel, stresses start to develop with the growth of the mechanical properties of the material. The main residual constraints finally appear after vitrification, during the cooling-down phase of the cycle.

Conclusion and prospects

The FEA model developed allows the distortions induced during the autoclave curing of M21EV/IMA laminates to be followed and simulated. The model established is made of various coupled modules describing the thermo-kinetic, thermo-chemical and thermo-mechanical behaviour of the material throughout the cure cycle. It is operational in 2D and 3D and can separate the strains according to their origins: thermal, chemical or mechanical. The model predicts the distortions of simple generic samples with a satisfactory accuracy. The next step of the model validation will be to compare the simulation results for large composite panels.

In the simulation tool developed, the influence of the mould on distortions is currently ignored. With the use of an INVAR mould, a releasing agent and an FEP release film, the impact of the mould interaction on the final distortions is not too great. However, for economic reasons, it could be very interesting to use a steel

or aluminium mould but these materials have CTEs that are much higher than those of the composite. The tool/part interaction will then have an important influence on the residual deformations of the parts. A more developed model is thus needed, to take account of the anisotropy of friction coefficient and also the variation of the shearing stress limit with the degree of composite cure. For this purpose, a model inspired from the work of Fiorina et al.[31,32] is being developed.

Declaration of Conflicting Interests

The author(s) declared no potential conflicts of interest with respect to the research, authorship, and/or publication of this article.

Funding

The author(s) disclosed receipt of the following financial support for the research, authorship, and/or publication of this article This study is part of the MAESTRIA project of the CORAC – Conseil pour la Recherche Aéronautique Civile, supervised and founded by the DGAC – Direction Générale de l'Aviation Civile and is undertaken as a part of a strong partnership with Dassault Aviation.

ORCID iD

Bruno Castanié https://orcid.org/0000-0002-2727-8622

References

1. Kappel E, Stefaniak D and Fernlund G. Predicting process-induced distortions in composite manufacturing – a pheno-numerical simulation strategy. *Compos Struct* 2015; 120: 98–106.
2. Stefaniak D, Kappel E, Spröwitz T, et al. Experimental identification of process parameters inducing warpage of autoclave-processed CFRP parts. *Compos Part A Appl Sci Manufact* 2012; 43: 1081–1091.
3. Olivier PA. A note upon the development of residual curing strains in carbon/epoxy laminates. Study by thermomechanical analysis. *Compos Part A Appl Sci Manufact* 2006; 37: 602–616.
4. Yu H, Mhaisalkar SG and Wong EH. Cure shrinkage measurement of nonconductive adhesives by means of a thermomechanical analyzer. *J Electron Mater* 2005; 34: 1177–1182.
5. Garstka T, Ersoy N, Potter KD, et al. In situ measurements of through-the-thickness strains during processing of AS4/8552 composite. *Composites Compos Part A Appl Sci Manufact* 2007; 38: 2517–2526.
6. Péron M, Cardinaud R, Lefèvre N, et al. PvT-HADDOC: a multi-axial strain analyzer and cure monitoring device for thermoset composites characterization during manufacturing. *Compos Part A Appl Sci Manufact* 2017; 101: 129–142.
7. Nawab Y. *Characterization and modelling of cure dependant properties of thermoset composites - Application to the simulation of residual stresses*. PhD Thesis - Génie Mécanique, Université de Nantes, France, 2012.
8. Minakuchi S, Niwa S, Takagaki K, et al. Composite cure simulation scheme fully integrating internal strain measurement. *Compos Part A Appl Sci Manufact* 2016; 84: 53–63.
9. Mulle M, Collombet F, Olivier P, et al. Assessment of cure residual strains through the thickness of carbon–epoxy laminates using FBGs, Part I: elementary specimen. *Compos Part A Appl Sci Manufact* 2009; 40: 94–104.
10. Parlevliet PP, Bersee HEN and Beukers A. Measurement of (post-)curing strain development with fibre Bragg gratings. *Polym Test* 2009; 29: 291–301.
11. Crasto AS and Kim RY. On the determination of residual stresses in fiber-reinforced thermoset composites. *J Reinf Plast Compos* 1993; 12: 545–558.
12. Johnston A. *An integrated model of the development of process-induced deformation in autoclave processing of composite structures*. PhD Thesis, The University of New Brunswick, Canada, 1997.
13. Ersoy N, Garstka T, Potter K, et al. Development of the properties of a carbon fibre reinforced thermosetting composite through cure. *Compos Part A Appl Sci Manufact* 2010; 41: 401–409.
14. Jakobsen J, Jensen M and Andreasen JH. Thermomechanical characterisation of in-plane properties for CSM E-glass epoxy polymer composite materials – Part 2: Young's modulus. *Polym Test* 2013; 32: 1417–1422.
15. Abou Msallem Y, Jacquemin F, Boyard N, et al. Material characterization and residual stresses simulation during the manufacturing process of epoxy matrix composites. *Compos Part A Appl Sci Manufact* 2010; 41: 108–115.
16. Ruiz E and Trochu F. Numerical analysis of cure temperature and internal stresses in thin and thick RTM parts. *Compos Part A Appl Sci Manufact* 2005; 36: 806–826.
17. Ruiz E and Trochu F. Thermomechanical properties during cure of glass-polyester RTM composites: elastic and viscoelastic modeling. *J Compos Mater* 2005; 39: 881–916.
18. Johnston A, Vaziri R and Poursartip A. A plane strain model for process-induced deformation of laminated composite structures. *J Compos Mater* 2001; 35: 1435–1469.
19. Kamal MR and Sourour S. Kinetics and thermal characterization of thermoset cure. *Polym Eng Sci* 1973; 13: 59–64.
20. Ledru Y. *Etude de la porosité dans les matériaux composites stratifiés aéronautiques*. PhD Thesis - Génie Mécanique, Mécanique et Matériaux, Univerté de Toulouse, France, 2009.
21. Paris C. *Étude et modélisation de la polymérisation dynamique de composites à matrice thermodurcissable*. PhD Thesis, INPT, http://ethesis.inp-toulouse.fr/archive/00001787/ (2011, accessed 4 March 2017).
22. Baran I, Cinar K, Ersoy N, et al. A review on the mechanical modeling of composite manufacturing processes. *Arch Comput Methods Eng* 2017; 24: 365–395.
23. Paris C, Bernhart G, Olivier P, et al. Influence de cycles de cuisson rapides sur le préimprégné aéronautique

M21/T700: suivi de polymérisation et propriétés mécaniques. In: *JNC 17*. Poitiers-Futuroscope: AMAC, 2011.
24. DiBenedetto AT. Prediction of the glass transition temperature of polymers: a model based on the principle of corresponding states. *J Polym Sci Part B Polym Phys* 1987; 25: 1949–1969.
25. Pascault JP and Williams RJJ. Relationships between glass transition temperature and conversion. *Polym Bull* 1990; 24: 115–121.
26. Pascault JP and Williams RJJ. Glass transition temperature versus conversion relationships for thermosetting polymers. *J Polym Sci Part B* 1990; 28: 85–95.
27. Nielsen LE. Cross-linking–effect on physical properties of polymers. *J Macromol Sci Part C* 1969; 3: 69–103.
28. Bogetti TA and Gillespie JW Jr. Process-induced stress and deformation in thick-section thermoset composite laminates. *J Compos Mater* 1992; 26: 626–660.
29. Khoun L. *Process-induced stresses and deformations in woven composites manufactured by resin transfer moulding*. PhD Thesis - Mechanical Engineering, McGill University, Canada, 2009.
30. Curiel T and Fernlund G. Deformation and stress build-up in bi-material beam specimens with a curing FM300 adhesive interlayer. *Compos Part A Appl Sci Manufact* 2008; 39: 252–261.
31. Fiorina M, Seman A, Castanie B, et al. Spring-in prediction for carbon/epoxy aerospace composite structure. *Compos Struct* 2017; 168: 739–745.
32. Mezeix L, Seman A, Nasir MNM, et al. Spring-back simulation of unidirectional carbon/epoxy flat laminate composite manufactured through autoclave process. *Compos Struct* 2015; 124: 196–205.